

Electron Spin and Its History

Eugene D. Commins

Physics Department, University of California, Berkeley, California 94720;
email: commins@berkeley.edu

Annu. Rev. Nucl. Part. Sci. 2012. 62:133–57

First published online as a Review in Advance on
May 15, 2012

The *Annual Review of Nuclear and Particle Science*
is online at nucl.annualreviews.org

This article's doi:
10.1146/annurev-nucl-102711-094908

Copyright © 2012 by Annual Reviews.
All rights reserved

0163-8998/12/1123-0133\$20.00

Keywords

g-value anomaly, quantum electrodynamics, spin magnetic dipole moment,
spin electric dipole moment

Abstract

The history of electron spin is summarized. Topics include the discovery of electron spin, the birth of quantum electrodynamics, the invention of magnetic resonance, the invention of renormalization, the anomalous magnetic moment of the electron in experiment and theory, and searches for the electron electric dipole moment.

Contents

1. INTRODUCTION	134
2. THE DISCOVERY OF ELECTRON SPIN	135
3. THE BIRTH OF QUANTUM ELECTRODYNAMICS	137
4. MAGNETIC RESONANCE	138
5. RENORMALIZATION	138
6. EXPERIMENTAL DETERMINATIONS OF a_e	139
6.1. Early Experiments	139
6.2. The Michigan $g - 2$ Experiments	139
6.3. The Seattle Penning Trap Experiment	140
6.4. The Harvard Penning Trap Experiment	144
7. OUTLINE OF THE THEORY OF a_e	144
8. COMPARISON OF EXPERIMENT AND THEORY FOR a_e	148
9. MUON $g - 2$ EXPERIMENT AND COMPARISON WITH THEORY	149
10. THE ELECTRON ELECTRIC DIPOLE MOMENT	150
10.1. Electric Dipole Moments and Violation of P and T Symmetries	150
10.2. Proper-Lorentz-Invariant, Gauge-Invariant Electric Dipole Moment Lagrangian Density	151
10.3. Electron Electric Dipole Moment Experimental Searches	152
11. CONCLUDING REMARKS ON SPIN	154

1. INTRODUCTION

In this article, we review the discovery of electron spin, summarize the remarkable experimental and theoretical efforts extending over decades to measure and understand the electron spin magnetic moment, and discuss the electron spin electric dipole moment (EDM), which has been sought for more than half a century but still eludes observation. Each of these topics has been treated many times in the literature. For example, the circumstances surrounding the discovery of electron spin are described in section 3.4 of Jammer's (1) excellent book, *The Conceptual Development of Quantum Mechanics*, and in *Theoretical Physics in the Twentieth Century: A Memorial Volume to Wolfgang Pauli*, edited by Fierz & Weisskopf (2). The latter book contains a chapter by Ralph Kronig, the first to discover electron spin, and another chapter by B.L. van der Waerden, who describes its rediscovery by George Uhlenbeck and Samuel Goudsmit. Uhlenbeck (3) and Goudsmit (4) also wrote about this historic event. The discovery of electron spin is also described by Tomonaga (5), one of the founders of renormalized quantum electrodynamics (QED), in his attractive book, *The Story of Spin*. A very clear and absorbing account of the development of renormalized QED and its relation to the anomalous magnetic moment of the electron is given by Schweber (6) in *QED and the Men Who Made It: Dyson, Feynman, Schwinger, and Tomonaga*. The recent book *Lepton Dipole Moments*, edited by Roberts & Marciano (7), contains 19 chapters by various authors on experimental and theoretical aspects of lepton dipole moments, including a chapter on the electron EDM. A separate review in this volume discusses the current status of the muon anomalous magnetic moment (8). In addition, there are many standard textbooks on quantum mechanics and quantum field theory, as well as countless research papers, review articles, and monographs, on experimental and theoretical topics related to electron (and muon) spin. Given such abundant literature, it may seem that this article is unnecessary. Nevertheless, I have

been persuaded to write it in the hope that a brief summary of the history of electron spin may be useful.

2. THE DISCOVERY OF ELECTRON SPIN

In 1921, Compton (9) suggested that electron spin would be an essential ingredient in any reasonable explanation of bulk paramagnetism and ferromagnetism. Unfortunately, Compton's proposal had almost no impact on his contemporaries; thus our story really begins in January 1925. At that time, quantum mechanics did not yet exist, and the generally accepted view of the atomic world was still classical, although it was supplemented by the partly successful but confusing quantization rules of the Bohr–Sommerfeld model. The anomalous Zeeman effect was a persistent puzzle that absorbed the attention of several physicists. Alfred Lande, who was in Tübingen, Germany, in 1925, had devised a useful and well-known semiempirical vector model to describe atomic angular momenta and the Zeeman effect (10), but how and why that model worked were a mystery.

Wolfgang Pauli also thought very carefully about the anomalous Zeeman effect, and his deep insight and wide knowledge of atomic spectra led him to formulate the exclusion principle at the end of 1924 (11). Having already attracted attention in 1921 at age 21 for his brilliant monograph on special and general relativity (12), confident of his own extraordinary abilities, and highly critical of others' work when it appeared superficial or naïve, Pauli would play an important role in the history of electron spin.

On January 7, 1925, the 20-year-old Kronig arrived in Tübingen on a traveling fellowship from Columbia University in New York to spend several weeks working with Lande, W. Gerlach, and E. Back. Lande greeted Kronig on his arrival, told him that Pauli would be visiting Tübingen the next day, and showed Kronig a letter from Pauli that he had just received. The letter emphasized that to understand the anomalous Zeeman effect, it would be necessary to endow the electron with a fourth quantum number in addition to the three it already possessed in the Bohr–Sommerfeld model, and that the fourth quantum number could take only two discrete values. On reading this letter, Kronig was immediately struck with inspiration, and that very afternoon he invented a concept of electron spin. His mental picture of the electron was of a tiny spinning classical sphere, and his interpretation of Pauli's fourth quantum number was that the spin axis could point in only two (opposing) directions. Because the sphere was charged as well as rotating, it must possess a magnetic moment. By choosing a value for the latter of one Bohr magneton (equivalent to $g_s = 2$ for a particle of spin 1/2 in modern notation), Kronig could understand the anomalous Zeeman effect, and he was able to construct a qualitative explanation for the doublet (D-line) splittings in the spectra of alkali atoms by means of the spin-orbit effect. With several hours remaining before an evening meeting with Lande, Kronig tested the latter idea quantitatively by calculating the fine structure splitting in what is now known as the 2^2p levels of atomic hydrogen. Here he ran into trouble: His calculation yielded a splitting twice as large as the observed value. Agreement could be obtained only if he assumed that in the spin-orbit effect the effective value of g_s is unity. Despite this obstacle, Kronig was elated by his success.

The next day Kronig explained his idea to Pauli, who praised it as a clever flash of wit but dismissed it as having no basis in reality. Pauli had two specific objections: the factor-of-two discrepancy in the hydrogen fine structure and the fact that if, as was widely believed, the electron was a sphere with the classical radius $r_0 = \frac{e^2}{m_e c^2}$, the surface velocity would be hundreds of times the velocity of light. More generally, Pauli certainly realized that the fourth quantum number corresponded to a classically nondescribable degree of freedom, so he must have viewed Kronig's classical picture of the electron as unacceptably naïve.

Kronig, who in later years described himself as very inexperienced at age 20, was undoubtedly crestfallen by Pauli's rejection. He resumed his travels after several weeks and eventually arrived at Niels Bohr's institute in Copenhagen, where he presented his idea again. Unfortunately, Bohr and others also gave it a cold reception, objecting on the same grounds as Pauli had. Now thoroughly disheartened, Kronig decided to abandon the idea of electron spin. In July 1925, Werner Heisenberg invented his version of quantum mechanics (matrix mechanics), which was greeted in Copenhagen as a great advance, but Kronig's spin seemed to have been forgotten.

The next development occurred in autumn 1925 in Leiden, Holland, where Uhlenbeck, 24, and Goudsmit, 23, were students of the professor of theoretical physics Paul Ehrenfest. According to Uhlenbeck's recollection, he and Goudsmit, unaware of Kronig's efforts, essentially reinvented the latter's idea in one afternoon. Excited by their achievement, the two went to Ehrenfest, who told them that it was either nonsense or something very important, that they should write up a short paper, and that all three would then consult Professor Hendrik Lorentz. The elderly Lorentz was the preeminent theoretical physicist in the Netherlands, universally respected for his great scientific achievements and profound knowledge. He listened courteously to Uhlenbeck and Goudsmit and told them he would think things over and give them his reply. Indeed, in several days, Lorentz did reply at length in a handwritten manuscript in which he gave a number of serious objections to Uhlenbeck and Goudsmit's proposal, all based on his deep knowledge of classical electrodynamics. Discouraged by Lorentz's criticism, Uhlenbeck and Goudsmit told Ehrenfest that they wished to withdraw their paper. However, Ehrenfest had already sent it to the publisher. He told Uhlenbeck and Goudsmit not to worry: They were young enough to be forgiven for their stupidity! The short paper was published in *Naturwissenschaften* in November 1925 (13), and an even shorter version, in English, appeared in *Nature* in February 1926 (14). As soon as Bohr and Heisenberg became aware of Uhlenbeck and Goudsmit's contribution, they had second thoughts—perhaps there was something to the idea after all, despite the factor-of-two discrepancy in the hydrogen fine structure. However, to Pauli the idea was still heresy, and he adamantly rejected it.

In early 1926, Erwin Schrödinger invented wave mechanics, and he later showed that it and Heisenberg's matrix mechanics are equivalent. Meanwhile, in February 1926, Llewellyn H. Thomas, a 23-year-old Londoner born to Welsh parents, was on a traveling fellowship at Bohr's institute in Copenhagen. Thomas was familiar with the mathematics of special relativity, and he realized that the spin-orbit effect described by Uhlenbeck and Goudsmit required a relativistic correction. Thomas did the calculation and discovered that the effective value of g_s in the spin-orbit effect is approximately unity, not two (15). Thus, the discrepancy between theory and experiment for the hydrogen fine structure disappeared. In March 1926, when Pauli learned of Thomas's result, he was converted to the idea of electron spin, and within about a year he developed a formalism for describing the spinning electron in nonrelativistic wave mechanics (16). Here, a two-component wave function is acted on not only by the Schrödinger Hamiltonian but also by what became known as the 2×2 Pauli spin matrices. Incidentally, a similar formalism was developed at about the same time by Charles G. Darwin (17), grandson of the great naturalist Charles Darwin.

Early in 1928, Paul A.M. Dirac, then 25, proposed his relativistic wave equation for the electron (18). From this equation, which is based on very general principles of Lorentz invariance, electron spin with $g_s = 2$ emerges naturally, along with what appeared to be a perfectly correct description of the fine structure in hydrogen, including the Thomas effect (19). Dirac's equation was too powerful and elegant to resist, and with its publication the idea of electron spin began to gain wide acceptance.

Ironically, just when Pauli was converted to electron spin, Kronig publicly rejected the notion (20) for the following reason. In August 1924, Pauli had proposed that the hyperfine structure

splittings observed in optical spectra of heavy atoms have their physical origin in the magnetic interaction between an atomic electron's orbital motion and a tiny magnetic moment of the nucleus (21). At the time, nuclei were thought to be composed of the only known particles: protons and electrons. Kronig argued that if the electron had a spin magnetic moment of one Bohr magneton, any nucleus with an odd number of electrons would also necessarily have a magnetic moment of the order of an electron Bohr magneton, approximately 1,000 times too large to explain observed hyperfine structure splittings. In his letter to *Nature* (20) in March 1926, Kronig wrote: "The new hypothesis. . . appears rather to effect the removal of the family ghost from the basement to the sub-basement, instead of expelling it definitely from the house."

Kronig's point seems sensible, given what was known at the time, and it is curious that Pauli did not voice the same objection. In any event, the problem resolved itself gradually. In 1927, the American physicist David Dennison, by analyzing existing data on the specific heat of hydrogen molecules at low temperatures, showed that the proton, like the electron, must have spin 1/2 and, thus, a spin magnetic moment of its own (22). (Dennison's analysis followed an earlier one by Hund, who had drawn erroneous conclusions.) Also in 1927, Goudsmit and Back, unaware of Pauli's 1924 paper on hyperfine structure, proposed the idea of nuclear spin to account for hyperfine splittings in bismuth (see Reference 23 and references therein). In 1930, Enrico Fermi employed Dirac's equation to obtain a precise formula for the hyperfine interaction between a nuclear magnetic moment and the spin magnetic moment of an atomic electron in an *S* state (24). Finally, and most importantly, Chadwick (25) discovered the neutron in 1932, which quickly led to a brief proposal by Iwenco (26), and a much more detailed independent proposal by Heisenberg (27), that complex nuclei consist of protons and neutrons, not protons and electrons.

3. THE BIRTH OF QUANTUM ELECTRODYNAMICS

We now turn to the small but important departure of g_s from two. This departure is caused mainly by quantum electrodynamic radiative effects and is frequently expressed in terms of the anomaly a_e , defined by $g_s = 2(1 + a_e)$ or, equivalently, $a_e = \frac{1}{2}(g_s - 2)$. QED was born in 1927 when Dirac (28) showed how to quantize the electromagnetic field. Obviously, this was an extremely important achievement, but in 1929–1930 Heisenberg & Pauli (29), Waller (30), and Oppenheimer (31) showed that QED contains UV divergences, including an infinite self-energy of the electron. This was an extremely serious problem: Whereas calculations of diverse quantum electrodynamic effects in the lowest order of perturbation theory made sense and could be compared with experiment, higher-order corrections yielded nonsensical infinities. This obstacle was not cleared away until the period between 1947 and 1951, when renormalization, the method for isolating and subtracting away the divergences, was invented.

Despite this problem, there were many significant advances in relativistic quantum mechanics and quantum field theory in the 1930s and early 1940s. In 1930, Dirac (32) attempted to overcome the difficulties associated with negative energies in his relativistic wave equation for the electron by proposing the hole theory. In its original version, the positive charges in hole theory were assumed to be protons, but when fundamental objections to that scheme were raised by Oppenheimer (33), Tamm (34), and others, Dirac (35) presented a revised version in 1931 in which the positive charges were positrons. The first observations of the positron in 1932–1933 by Anderson (36) and by Blackett & Occhialini (37) helped Dirac's new theory of positrons gain acceptance. The hole theory itself was recast in 1933–1934 into an equivalent description involving the quantized electron-positron field, in independent works by Fock (38), Furry & Oppenheimer (39), and Heisenberg (40). The concept of vacuum polarization, which arises naturally in hole theory, was introduced by Dirac (41) in 1933, developed by Heisenberg and his students in 1934–1935, and

simplified and given a clear physical explanation by Weisskopf (42) in 1936. In 1935, Uehling (43) calculated the effect of vacuum polarization on the energy levels of atomic hydrogen. The very important result—that in hole theory or its equivalent field-theoretic formulation the self-energy of the electron has only a logarithmic UV divergence—was first established by Weisskopf (44) in 1934; his result was refined by Furry & Oppenheimer (39), and a more complete analysis was presented by Weisskopf (45) in 1939. Other very fruitful applications of quantum field theory included Fermi’s (46) theory of nuclear β decay, published in 1934, and Yukawa’s (47) meson theory of nuclear forces, published in 1935. Pauli (48) completed the earlier work of Fierz and others by establishing the field-theoretic connection between spin and statistics in 1940. All of these achievements were highly significant, but the UV divergences in quantum field theory, and specifically in QED, remained a fundamental obstacle until after World War II.

4. MAGNETIC RESONANCE

On the experimental side, until the 1930s, only very crude precision could be achieved in measurements of spin-related phenomena such as nuclear magnetic moments, Zeeman energies, and hyperfine structure splittings because of the limitations of existing laboratory techniques. However, this situation began to change in 1937, when Rabi (49) invented magnetic resonance at Columbia University. Rabi had visited Otto Stern’s Hamburg laboratory in the 1920s and was strongly influenced by Stern. Immanuel Estermann and Stern had been the first to measure the proton spin magnetic moment, which they achieved by using a beam of H_2 molecules and employing the Stern–Gerlach magnetic deflection method (50). In 1938, Rabi and coworkers (51) combined the Stern–Gerlach technique with magnetic resonance in an atomic/molecular beam radio-frequency (RF) spectrometer, which was capable of vastly greater precision than had ever been obtained before. With this new technique, Rabi and his group performed many outstanding experiments, including a very precise measurement of the proton magnetic moment (52), before the onset of World War II interrupted research everywhere.

5. RENORMALIZATION

Research resumed at Columbia in 1946; RF and microwave technology had greatly expanded in the meantime because of wartime radar development, which enabled two separate experiments that had momentous consequences. The first was an atomic beam measurement of the hyperfine structure splitting in the ground state of hydrogen; this study was carried out by two of Rabi’s students, John Nafe and Edward Nelson (53). It was expected that this experiment would verify the prediction derived from Fermi’s formula for this splitting:

$$\Delta\nu_{\text{predicted}}(^1\text{H}, 1^2s_{1/2}) = 1,416.97(0.54) \text{ MHz},$$

which was calculated from $g_s = 2$ for the electron, the known proton magnetic moment [determined assuming $g_s = 2$ (52)], and the known value of the ground-state electronic wave function at the nucleus. However, Nafe & Nelson obtained the result

$$\Delta\nu_{\text{observed}}(^1\text{H}, 1^2s_{1/2}) = 1,420.410(0.006) \text{ MHz},$$

which was corroborated in an MIT experiment by Zacharias and coworkers (54). An explanation for the discrepancy was soon suggested by Breit (55): g_s might be slightly larger than two, in disagreement with the Dirac theory. The second experiment was a measurement of the energy separation between the metastable $2s_{1/2}$ state and the short-lived $2p_{1/2}$ state in hydrogen,

performed with an atomic beam–microwave technique invented by Willis Lamb. According to Dirac’s theory, these two states should be degenerate, but in a beautiful measurement Lamb & Retherford (56) found a relative shift of 1,058 MHz—now known as the Lamb shift.

Almost immediately, researchers suggested that these two experimental results were related to the UV divergence problems in QED, thereby providing a powerful stimulus for theoretical physicists to give explanations. Hans Bethe (57) made the first advance in June 1947 by working out the essential theory of the Lamb shift. Bethe’s renormalization calculation was nonrelativistic and thus not complete, but it was soon followed by more complete relativistic treatments of the Lamb shift, done independently by French & Weisskopf (58), Kroll & Lamb (59), Tomonaga (60), Richard Feynman, Julian Schwinger, and others.

At the end of 1947, Schwinger succeeded in calculating the lowest-order quantum electrodynamic correction to g_s (61). He obtained the result

$$a_e = \frac{\alpha}{2\pi} + \dots,$$

where $\alpha = \frac{e^2}{\hbar c}$ is the fine structure constant. This result accounted for the discrepancy found by Nafe & Nelson, and it also agreed with the first direct determination of a_e , which was obtained from measurements of the Zeeman effect in the $^2p_{1/2,3/2}$ states of gallium and the $^2s_{1/2}$ state of sodium by Kusch & Foley (62), done shortly after Nafe & Nelson’s result was obtained.

Two general theoretical approaches to renormalization in QED appeared at approximately the same time: one created by Feynman (63) and the other developed independently by Schwinger (64) and Tomonaga (60). At first, the Feynman and Schwinger–Tomonaga methods seemed different, but in 1949 Dyson (65) proved that they are equivalent. Dyson (66), Salam (67), and Ward (68) also showed that once renormalization is achieved, no further infinities are encountered in higher-order radiative corrections. These early achievements were the first in what became a six-decade development of experiment and theory yielding steadily increasing accuracy in the determination of g_s . We now summarize this development, starting with the electron experiments.

6. EXPERIMENTAL DETERMINATIONS OF a_e

6.1. Early Experiments

Figure 1 is a plot of the fractional uncertainty in a_e obtained experimentally between 1948 and 2008. It shows an increase in precision over the past six decades of approximately eight orders of magnitude. In the first measurements, done at Columbia by Kusch and coworkers, the atomic beam magnetic resonance method was employed to observe the Zeeman effect, first in gallium and sodium as mentioned above (62) and then in atomic hydrogen (69). In the latter case, the magnetic field was determined by an auxiliary NMR measurement of the proton magnetic moment in a sample of mineral oil; thus, the Columbia group actually determined the quantity g_s/g_p , where g_p is the proton spin g value. Subsequently, a microwave absorption experiment at Yale by Beringer & Heald (70) obtained a consistent result for g_s/g_p . However, the quantity of interest was g_s/g_ℓ , where $g_\ell (=1)$ is the electron orbital g value; therefore, it was necessary to rely on the result of a separate measurement of g_p/g_ℓ by Gardner & Purcell (71) at Harvard. For a time there was considerable confusion when an error was discovered in the Gardner–Purcell result (72).

6.2. The Michigan $g - 2$ Experiments

The fundamental limitations of these early experiments were overcome, and substantial improvements in precision were achieved by H. Richard Crane, Arthur Rich, and their coworkers at the

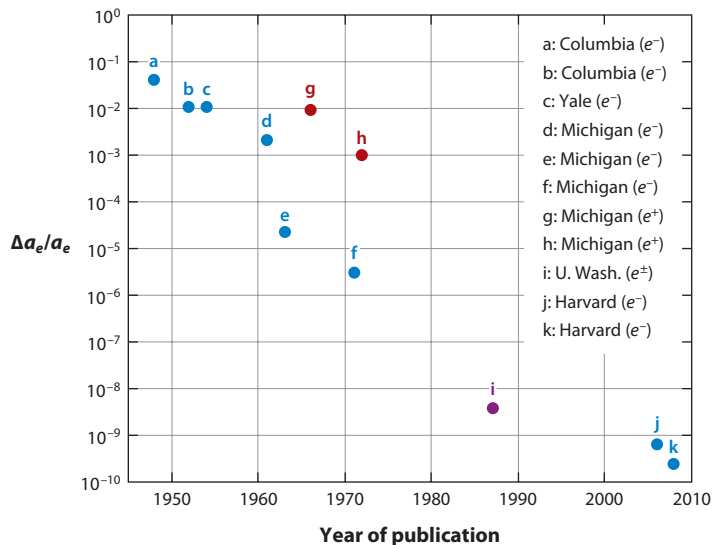


Figure 1

Experimentally determined fractional uncertainty in a_e , plotted versus year of publication. Plots correspond to references as follows: a, 62; b, 69; c, 70; d, 73; e, 74; f, 75; g, 76; h, 77; i, 78; j, 80; k, 81. The blue and red dots refer to electron and positron measurements, respectively. The purple dot indicates that the measurement was done separately with electrons and positrons, both of which gave the same result.

University of Michigan. These researchers employed the basic principle that in a magnetic field \mathbf{B} , the spin precession angular velocity $\boldsymbol{\omega}_s$ and the cyclotron angular velocity $\boldsymbol{\omega}_c$ of a free particle of mass m and charge q differ by a factor proportional to a :

$$\boldsymbol{\omega}_s = -g \frac{q}{2m} \mathbf{B} - \frac{q}{\gamma m} (1 - \gamma) \mathbf{B},$$

$$\boldsymbol{\omega}_c = -\frac{q}{m\gamma} \mathbf{B},$$
1.

$$\boldsymbol{\omega}_a = \boldsymbol{\omega}_s - \boldsymbol{\omega}_c = -\left(\frac{g-2}{2}\right) \frac{q}{m} \mathbf{B} = -a \frac{q}{m} \mathbf{B},$$

where, as usual, $\gamma = (1 - v^2/c^2)^{-1/2}$. In the Michigan electron experiments, a beam of unpolarized electrons of energy ≈ 100 keV underwent Mott scattering on a foil and thus became partially polarized (73–75). In a magnetic field, the scattered polarized beam moved into a central region, where the electrons became trapped in a potential well for a time T . Subsequently, the electrons were extracted, underwent Mott scattering again to analyze their polarization, and were detected. From the sinusoidal dependence of the signal on T , the frequency ω_a and thus the anomaly a of a free electron were measured directly. A modified version of this experiment was used to determine a for free positrons (76, 77). These positrons were obtained from a ^{58}Co source and were emitted with longitudinal polarization $\mathcal{P} = \frac{v}{c}$; therefore, Mott scattering was not necessary for initial polarization.

6.3. The Seattle Penning Trap Experiment

Dramatic improvements in measurements of a for e^\pm were made in the 1980s by Dehmelt and coworkers (78) at the University of Washington, Seattle. A single electron and, separately, a single

positron were suspended for months in a magnetic field B_z , and the frequencies $\omega_d = \omega_s - \omega_c$ and ω_c were measured repeatedly. The suspension was achieved by means of a Penning trap with electrostatic potential

$$\phi(r, z) = U_0 \left[\frac{r^2 - 2z^2}{4Z_0^2} + D_4 \frac{8z^4 - 24r^2z^2 + 3r^4}{16Z_0^4} + \dots \right] \quad 2.$$

generated by electrodes in the shape of hyperboloids of revolution. Here, $\phi(r, z)$ is expressed in cylindrical polar coordinates, and U_0 , Z_0 , and D_4 are constants. The term containing D_4 on the right-hand side of Equation 2 represents a correction arising from imperfections and misalignment of the hyperbolic electrodes, and was very small compared with the first term; for many purposes this term can be neglected. Also, the potentials for the electron and positron measurements differed only in the sign of U_0 .

In the combined magnetic and electric fields, an electron or positron has three spatial components of motion in addition to its spin precession: axial motion along z , cyclotron motion, and magnetron motion. A RF electric field was applied to drive the axial motion, and microwave and RF fields were employed to induce cyclotron and anomaly transitions, respectively; we first discuss the axial, cyclotron, and magnetron motions in the absence of these oscillating fields. If we neglect the term in D_4 on the right-hand side of Equation 2, the axial force on an electron (with charge $-e$) is

$$F_e^z = e \frac{\partial \phi}{\partial z} = -\frac{eU_0z}{Z_0^2}. \quad 3.$$

Therefore, in a uniform magnetic field B_0 in the z direction, the simple harmonic oscillation frequency of axial motion would be given by $\omega_{z0}^2 = \frac{e}{m} \frac{U_0}{Z_0^2}$. However, a weak axial gradient in the magnetic field was deliberately imposed:

$$B_z = B_0 + \beta z^2, \quad \beta z^2 \ll B_0,$$

where $\beta \approx 150 \text{ Gcm}^{-2}$. Thus, the magnetic energy $U_M = -\mu \mathbf{B}$ for spin or cyclotron motion had the additional contribution on or near the center axis, $U'_M = -\mu_z \beta z^2$, which gives an additional force:

$$F_M^z = -\frac{\partial U'_M}{\partial z} = 2\mu_z \beta z. \quad 4.$$

The total restoring force is obtained by combining Equations 3 and 4:

$$F_{\text{total}}^z = -\left(\frac{eU_0}{Z_0^2} - 2\mu_z \beta \right) z.$$

The axial frequency is given by

$$\omega_z^2 = \omega_{z0}^2 - \frac{2\beta}{m} \mu_z. \quad 5.$$

Because the second term on the right-hand side of Equation 5 is much smaller than the first term, we may write ω_z to sufficient accuracy as

$$\omega_z = \omega_{z0} - \frac{\beta \mu_z}{m_0 \omega_{z0}}$$

or

$$v_z = v_{z0} - \frac{\beta \mu_z}{2\pi m_0 \omega_{z0}} = v_{z0} - \delta v. \quad 6.$$

Thus, a change in the cyclotron and/or spin quantum numbers, which causes a change in the electron magnetic moment, also results in a change in the axial frequency. This change was the basis

for detection of the cyclotron and anomaly frequencies. In the Seattle experiment, $\nu_{z0} \approx 60$ MHz, and $\delta\nu \approx (1.3 \pm 0.2)$ Hz for μ_z equal to one Bohr magneton.

Axial motion of the charge in the space between the electrodes generated an image current in a circuit containing the electrodes and an external resistor R_0 , all maintained at a temperature of 4.2 K. The axial motion was thus in thermal equilibrium with R_0 , and the Johnson noise voltage of this resistor gave rise to white noise fluctuations in the axial motion. As mentioned above, a RF electric field was also applied to drive the axial motion at the frequency ν_z .

If the trapping electric field were zero, the cyclotron motion in a uniform magnetic field would be described quantum mechanically by the usual harmonic oscillator-like levels, which are characterized by the quantum number $n = 0, 1, 2, \dots$ and the frequency splitting ω_c , as in Equation 1. However, as we discuss below, ω_c was altered slightly in the presence of the trapping electric field by a correction for magnetron motion. Equilibrium between the cyclotron motion and the thermal bath was maintained by synchrotron radiation between cyclotron levels, with a mean lifetime for spontaneous emission of ≈ 1 s (inhibited by approximately a factor of 10 through the presence of the Penning trap cavity). In the Seattle experiment, where $B_z \approx 5$ T, $\nu_c = \omega_c/2\pi \approx 140$ GHz. Therefore, at 4.2 K, only a few cyclotron levels were populated, and the probability for finding the charge in the $n = 0$ cyclotron level was approximately 0.8 in the absence of stimulated absorption from the external microwave source.

The magnetron motion (so weakly coupled to the thermal bath that it was never close to thermal equilibrium) may be understood most simply by considering classical circular motion about the center axis. Neglecting the term in D_4 on the right-hand side of Equation 2, we have

$$E_r = -\frac{\partial\phi}{\partial r} = -\frac{U_0 r}{2Z_0^2}.$$

The radial electric force on an electron is

$$F_r = -eE_r = \frac{eU_0 r}{2Z_0^2}.$$

If we neglect the small magnetic field gradient, the Lorentz force in the magnetic field is

$$F_r' = -e\frac{v}{c}B_0 \quad (\text{directed toward the axis}).$$

Thus, from Newton's law,

$$m\omega^2 r = \frac{e\omega r}{c}B_0 - \frac{m}{2}\omega_{z0}^2 r, \quad 7.$$

where ω is the angular frequency of circular motion. Equation 7 may be written as

$$\omega^2 - \omega_c \omega + \frac{1}{2}\omega_{z0}^2 = 0,$$

the solutions of which are

$$\omega_+ = \frac{\omega_c}{2} + \frac{1}{2}\sqrt{\omega_c^2 - 2\omega_{z0}^2} \approx \omega_c - \frac{\omega_{z0}^2}{2\omega_c} \quad 8.$$

and

$$\omega_- = \frac{\omega_c}{2} - \frac{1}{2}\sqrt{\omega_c^2 - 2\omega_{z0}^2} \approx \frac{\omega_{z0}^2}{2\omega_c}.$$

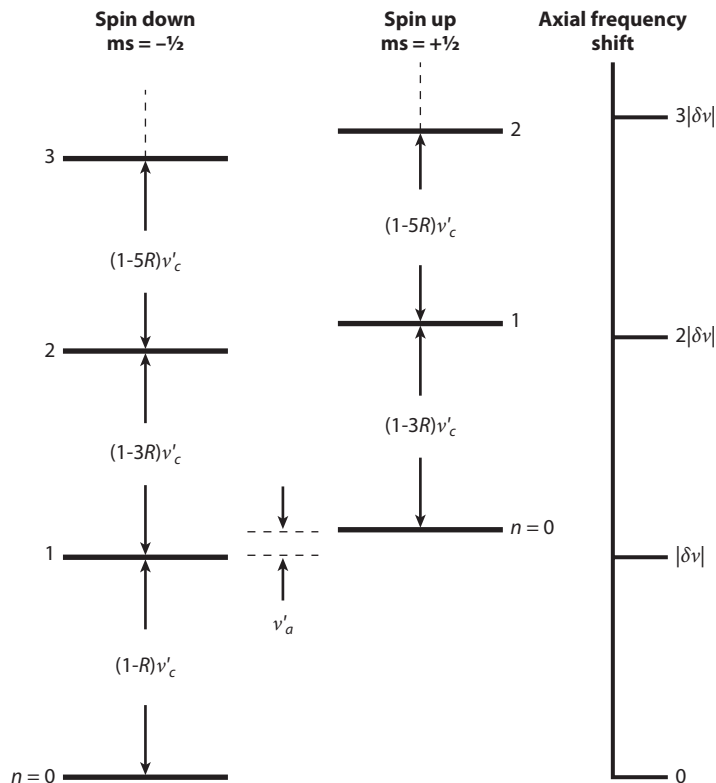


Figure 2

Energy levels of cyclotron motion and spin precession (not to scale) in the Seattle experiment (78). R is an extremely small relativistic correction; it and the corrected anomaly frequency ν'_a are greatly exaggerated for pictorial clarity.

The quantity $\omega_+ = \omega'_c$ was the observed cyclotron frequency in the Penning trap, whereas $\omega_- = \omega_M \ll \omega_+$ was the magnetron drift frequency. From Equation 8, it follows that

$$a = \frac{\omega_a}{\omega_c} = \frac{\omega_s - \omega_c}{\omega_c}$$

could be expressed to sufficient accuracy in terms of observed quantities as follows:

$$a = \frac{\omega'_a - \frac{\omega_s^2}{2\omega'_c}}{\omega'_c + \frac{\omega_s^2}{2\omega'_c}},$$

where $\omega'_a = \omega_s - \omega'_c$.

Figure 2 is a simplified energy-level diagram in which the energies of axial and magnetron motion are ignored, but the spin and cyclotron energies (with quantum numbers m and n , respectively) and also the shift in axial frequency described in Equation 6 are included. By application of the cyclotron microwave field and/or the anomaly RF field to induce transitions between various levels, and by observation of the corresponding axial frequency shifts, $a(e^-)$ and $a(e^+)$ were determined (for a careful analysis of the line shapes of anomaly and cyclotron resonances, see Reference 79). The results of this beautiful and subtle experiment, for which Dehmelt earned a

share of the 1989 Nobel Prize in Physics, are as follows:

$$a(e^-) = 1.159\,652\,188\,4(43) \times 10^{-3}, \quad 9.$$

$$a(e^+) = 1.159\,652\,187\,9(43) \times 10^{-3} \quad 10.$$

which yield

$$\frac{g(e^-)}{g(e^+)} = 1 + (0.5 \pm 2.1) \times 10^{-12}.$$

The latter is a sensitive test of *CPT* (charge–parity–time reversal) invariance, which requires that the g values of a particle and its corresponding antiparticle be the same: $g(e^-) = g(e^+)$.

6.4. The Harvard Penning Trap Experiment

The most recent measurements of a_e for the electron were made by Gabrielse and coworkers (80, 81) at Harvard. The basic experimental method here was similar to that employed at Seattle, but the Harvard group employed many important improvements, including the following:

1. The system was maintained at 0.1 K instead of 4.2 K. Thus, in thermal equilibrium, the probability of finding the electron in its ground cyclotron state was very nearly unity, rather than 0.8. The lower temperature resulted in much sharper definition of various resonances.
2. A cylindrical Penning trap, rather than hyperbolic electrodes, was used (**Figure 3**). The mode structure of the cavity, which could be calculated and was well understood, permitted precise and significant corrections for cavity shifts in cyclotron resonances and resulted in strong inhibition of spontaneously emitted synchrotron radiation, which would otherwise have caused an excessively short mean lifetime for cyclotron states excited by stimulated microwave absorption. Cavity inhibition of spontaneous emission also resulted in narrow line widths of measured resonances. Although the cavity was cylindrical, use of compensation electrodes allowed shaping of the electrostatic potential so that it closely approximated the first term on the right-hand side of Equation 2.
3. The use of modern electronic technology permitted very sophisticated automatic control of various experimental parameters.

The result of the Harvard experiment is

$$a_e^{\text{exp}} = 1.159\,652\,180\,73(28) \times 10^{-3}, \quad 11.$$

which represents a factor-of-15 improvement in precision compared with Equation 9. There is a discrepancy between Equations 9 and 11 at the 1.8- σ level.

7. OUTLINE OF THE THEORY OF a

We now summarize the theory of a for the electron, and also for the muon. There are three separate contributions to a :

$$a = a^{\text{QED}} + a^{\text{hadrons}} + a^{\text{electroweak}}.$$

By far the largest term is a^{QED} , which is expressed as a power series in $\alpha/\pi = 0.00232\dots$:

$$a^{\text{QED}} = C_2 \left(\frac{\alpha}{\pi}\right) + C_4 \left(\frac{\alpha}{\pi}\right)^2 + C_6 \left(\frac{\alpha}{\pi}\right)^3 + C_8 \left(\frac{\alpha}{\pi}\right)^4 + C_{10} \left(\frac{\alpha}{\pi}\right)^5 + \dots \quad 12.$$

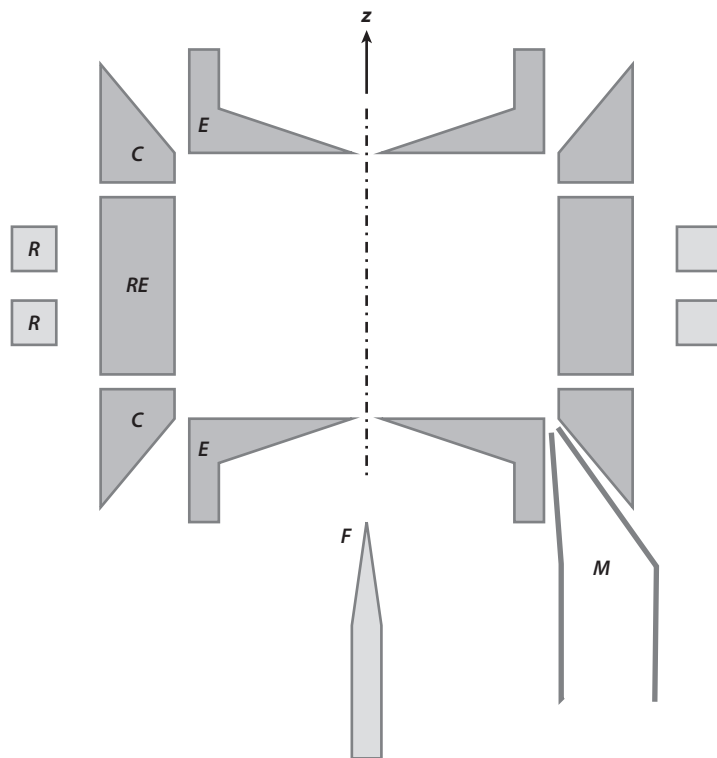


Figure 3

Simplified diagram of the Harvard cylindrical Penning trap (not to scale) (80, 81). Abbreviations: *E*, end-cap electrodes; *C*, compensation electrodes; *RE*, ring electrodes; *R*, nickel rings for generating magnetic field gradient; *F*, field emission point used to generate electrons; *M*, microwave input.

The coefficients C_n in Equation 12 are found by summing the renormalized amplitudes from all QED Feynman diagrams of order n for scattering of an electron or a muon by a static magnetic field. By QED, we mean that the internal lines in a diagram are limited to the photon and the charged leptons: (e , μ , τ).

Figure 4 shows the diagrams for zeroth, second, and fourth orders. In fourth order, a vacuum polarization diagram appears with an internal fermion-antifermion loop, and such loops also appear for $n = 6, 8, 10, \dots$. Because the amplitude for vacuum polarization depends on the mass of the particle (electron or muon), the g value of which is desired, the quantities $C_{n,e}$ and $C_{n,\mu}$ for $n \geq 4$ are not the same. The fourth-order correction for the electron was first calculated in 1950 by Karplus & Kroll (82); unfortunately their calculation was in error. The calculation was done correctly by Petermann (83) and independently by Sommerfield (84) in 1957–1958. For the muon, the fourth-order correction was first calculated by Suura & Wichmann (85) and independently by Petermann (86) in 1957.

As the order n increases, the number of diagrams increases rapidly, and so does the complexity of calculation associated with each diagram. In sixth order, there are 72 diagrams (**Figure 5**). The diagrams are so numerous that we simply show representatives of the various types. In addition to so-called q-type and vacuum polarization diagrams, which are qualitatively similar to analogous diagrams in fourth order, there are new “light-by-light” diagrams. It required many years of sustained effort by Laporta & Remiddi (87, 88) to calculate the entire sixth-order correction

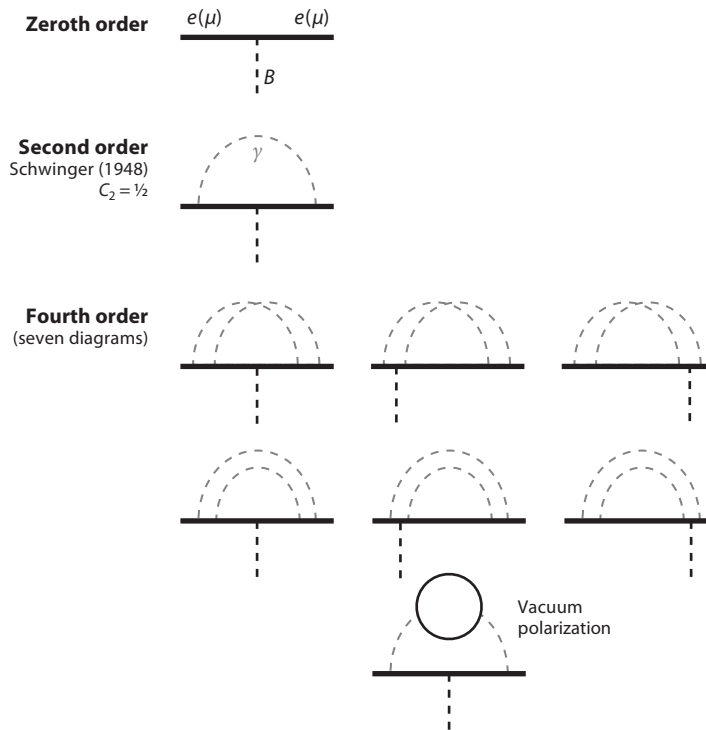


Figure 4

Zeroth-, second-, and fourth-order Feynman diagrams for a^{QED} .

analytically. Kinoshita (89, 90) performed the same calculation numerically through Monte Carlo evaluations of the multidimensional integrals associated with the various diagrams.

In eighth order, there are 891 diagrams; in tenth order, there are 12,672. Kinoshita and collaborators (91) have completed the eighth-order calculations numerically for the electron and muon. The same researchers have also calculated the most significant tenth-order terms for the muon (92) and many tenth-order terms for the electron (93). These extremely demanding calculations require great patience and skill and would be impossible without sophisticated computer programs for Feynman diagram algebra and multidimensional numerical integration, executed on high-speed computers.

The contributions to a^{hadrons} arise from diagrams of the vacuum polarization (94, 95) and light-by-light (96–98) types, in which the internal loops consist of strongly interacting particles such as π^+ and π^- (**Figure 6**). It is not possible to calculate such terms directly from quantum chromodynamics because the momentum transfer here is quite small. However, in the case of vacuum polarization, one can use dispersion theory to relate the dominant lowest-order contribution to an integral over the cross section for $e^+e^- \rightarrow \text{hadrons}$:

$$a_{\mu}^{\text{hadrons}}(\text{vacuum polarization, lowest order}) = \frac{1}{4\pi^3} \int_{4m_{\pi}^2}^{\infty} K_{\mu}(s) \sigma(e^+e^- \rightarrow \text{hadrons}) ds,$$

where

$$K_{\mu}(s) = \int_0^1 \frac{y^2(1-y)}{y^2 + \frac{s}{m_{\pi}^2}(1-y)} dy,$$

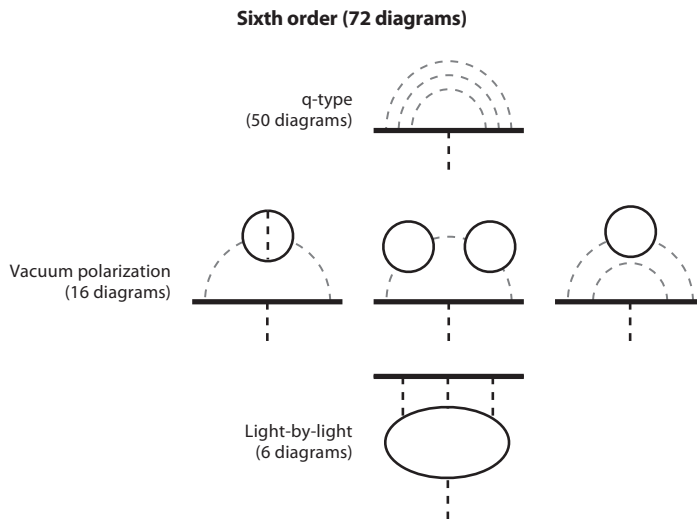


Figure 5

Representative sixth-order Feynman diagrams for a^{QED} .

and s is the square of the center-of-mass energy of e^- and e^+ . The cross section $\sigma(e^+e^- \rightarrow \text{hadrons})$ is determined experimentally, either from direct measurements as a function of s or by relating $\sigma(e^+e^- \rightarrow \text{hadrons})$ to

$$\Gamma(\tau \rightarrow \nu_\tau \pi^- \pi^0) / \Gamma(\tau \rightarrow \nu_\tau \bar{\nu}_e e^-).$$

The latter relation would hold strictly if isospin symmetry were perfect; however, it is imperfect, so corrections must be made. Importantly, the hadronic effects for a_μ are approximately $(\frac{m_\mu}{m_e})^2 \approx 4 \times 10^4$ times as large as for a_e .

The quantity $a^{\text{electroweak}}$ arises from diagrams in which photon internal lines are at least partly replaced by Z^0 , W^\pm , and/or Higgs boson lines; charged lepton internal lines are replaced by neutrino lines where necessary (Figure 7) (99; see Reference 100 for one-loop corrections and Reference 101 for two-loop electroweak contributions). One might think that single-loop electroweak diagrams would greatly dominate over those with two loops, but the latter actually make a relatively substantial contribution. For $a^{\text{electroweak}}$, the overall effect for the muon is once again approximately 4×10^4 times as large as for the electron.

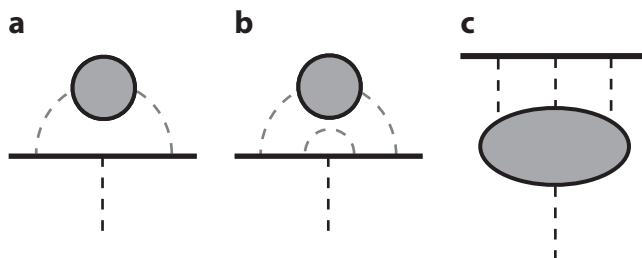


Figure 6

Examples of diagrams contributing to a^{hadrons} . (a) Lowest-order vacuum polarization diagram. (b) Next-order vacuum polarization diagram. (c) Lowest-order light-by-light diagram. The shaded blobs represent hadrons such as $\pi^+ \pi^-$.

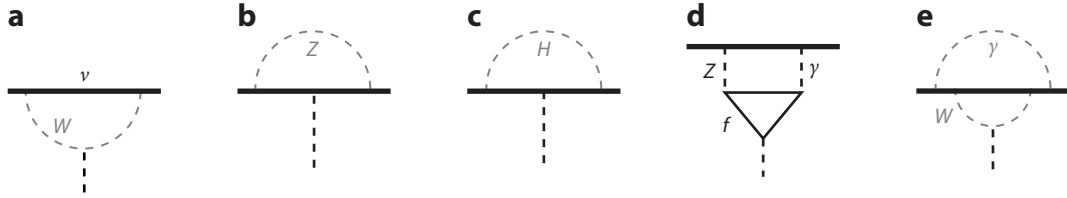


Figure 7

Examples of diagrams contributing to $a_e^{\text{electroweak}}$. (a–c) Single-loop diagrams. (d,e) Double-loop diagrams. Abbreviations: f , charged lepton or quark; H , Higgs boson.

8. COMPARISON OF EXPERIMENT AND THEORY FOR a_e

The theoretical results for a_e are as follows:

$$\begin{aligned}
 C_2^e &= 0.5, \\
 C_4^e &= -0.328\,478\,444\,002\,90 \quad (60), \\
 C_6^e &= 1.181\,234\,016\,827 \quad (19), \\
 C_8^e &= -1.914\,4(35), \\
 C_{10}^e &= 0.0 \quad (4.6), \\
 a_e^{\text{hadrons}} &= 1.682 \quad (20) \times 10^{-12}, \\
 a_e^{\text{electroweak}} &= 3.0 \quad (0.1) \times 10^{-14}.
 \end{aligned} \tag{13}$$

Note that although the coefficients $C_{4,6}^e$ have been evaluated analytically, they nevertheless have small uncertainties, which arise primarily from the experimental uncertainty in the ratio m_e/m_μ . An analogous comment holds for the coefficients C_n^μ for $n \geq 4$.

Because

$$a = C_2 \left(\frac{\alpha}{\pi} \right) + C_4 \left(\frac{\alpha}{\pi} \right)^2 + C_6 \left(\frac{\alpha}{\pi} \right)^3 + C_8 \left(\frac{\alpha}{\pi} \right)^4 + C_{10} \left(\frac{\alpha}{\pi} \right)^5 + \dots + a^{\text{hadrons}} + a^{\text{electroweak}},$$

it is obvious that for a precise comparison between theory and experiment one needs an accurate value of α in addition to the coefficients C_n^e , a_e^{hadrons} , and $a_e^{\text{electroweak}}$. In the past, α was best determined from the hyperfine splitting in muonium, by the Josephson effect, or by other methods. However, at present an independent determination of α is most precisely achieved from the relation

$$\alpha^2 = \frac{4\pi}{c} R_\infty \frac{\hbar}{m_e},$$

where R_∞ is the Rydberg constant for infinite nuclear mass. No accurate direct measurement of $\frac{\hbar}{m_e}$ exists, but we can write

$$\frac{\hbar}{m_e} = \frac{\hbar}{M_X} \frac{12M_X}{M(^{12}\text{C})} \frac{M(^{12}\text{C})}{12m_e}.$$

Here, $\frac{12m_e}{M(^{12}\text{C})}$ is the electron mass in atomic mass units (amu), $\frac{12M_X}{M(^{12}\text{C})}$ is the mass of X (a cesium or rubidium atom) in amu, and $\frac{\hbar}{M_X}$ is measured in an atom interferometer experiment, where an optical frequency and an atom recoil velocity are determined for cesium (102) or rubidium (103). One must also determine R_∞ from observed transition frequencies in atomic hydrogen, which requires theoretical corrections for proton recoil, proton size, and QED self-energy and vacuum polarization effects. The results for rubidium and cesium are

$$\alpha^{-1}(\text{Rb}) = 137.035\,999\,45 \quad (62) \quad (4.5 \text{ ppb}) \tag{14}$$

and

$$\alpha^{-1}(\text{Cs}) = 137.036\,000\,00 \text{ (110)} \quad (8.0 \text{ ppb}). \quad 15.$$

Alternatively, one can assume that the theory yielding the coefficients in Equation 13 is correct (104) and combine a_e^{exp} in Equation 11 with a_e^{theor} to obtain the value

$$\alpha^{-1}(a_e) = 137.035\,999\,085 \text{ (51)} \quad (0.37 \text{ ppb}). \quad 16.$$

The latter value agrees with Equations 14 and 15, but its uncertainty is approximately an order of magnitude smaller. The agreement indicates that the theory of a_e is correct to at least eighth order in a_e^{QED} . This is a truly remarkable achievement, although it is important to note that substantial QED calculations are required to determine R_∞ for the results given in Equations 14 and 15.

Clearly, a better independent determination of α is greatly desired. In the future, this determination could be obtained by comparing laser-atomic beam measurements of the fine structure splitting of the $1s2p\ ^3P$ multiplet in atomic helium with the theory of that splitting (105). The combination of a recent measurement by Smiciklas & Shiner (106) with theoretical calculations (107) to order $m_e\alpha^7$ yielded the result

$$\alpha^{-1} = 137.035\,999\,55 \text{ (64)} \quad (5 \text{ ppb}), \quad 17.$$

which agrees with Equations 14–16. However, an estimate of the dominant terms of order $m_e\alpha^8$, which has not yet been calculated in detail, enlarges the uncertainty in Equations 17 to 20 ppb.

9. MUON $g - 2$ EXPERIMENT AND COMPARISON WITH THEORY

Because a detailed review of a_μ appears elsewhere in this volume (8), we give only a very brief summary here. In the most recent experiment (Brookhaven E821), the proton beam of Brookhaven National Laboratory's Alternating Gradient Synchrotron was used to generate pions, which decayed in flight to produce a beam of longitudinally polarized muons with an average energy of 3.15 GeV (108, 109). The polarized muons were inflected into a storage ring with a diameter of 7.1 m. As a polarized muon circulated in the ring, its polarization precessed with frequency ω_μ relative to its momentum. When the muon decayed, it emitted an electron with an angular distribution relative to the muon polarization given by the $V-A$ law of charged weak interaction. Thus, with electron detectors placed around the ring, a plot of the electron signal versus time for well-defined initial muon bunches yielded a modulated decaying exponential, where the modulation provided information about a_μ . The result is

$$a_\mu^{\text{exp}} = 116\,592\,083 \text{ (63)} \times 10^{-11}, \quad 18.$$

which includes a very small correction for the ratio of muon and proton magnetic moments. Compare this result with

$$a_\mu^{\text{theor}} = 116\,591\,828 \text{ (49)} \times 10^{-11}, \quad 19.$$

which is obtained from the coefficients

$$\begin{aligned} C_2^\mu &= 0.5, \\ C_4^\mu &= 0.765857410 \text{ (37)}, \\ C_6^\mu &= 24.05050964 \text{ (43)}, \\ C_8^\mu &= 130.8055 \text{ (80)}, \\ C_{10}^\mu &= 663 \text{ (20)}, \\ a_\mu^{\text{hadrons}} &= 6.956 \text{ (49)} \times 10^{-8}, \\ a_\mu^{\text{electroweak}} &= 1.54 \text{ (02)} \times 10^{-9}, \end{aligned}$$

and the value of α given in Equation 16 (110). As mentioned above, $a_\mu^{\text{hadrons}}/a_e^{\text{hadrons}} \approx a_\mu^{\text{electroweak}}/a_e^{\text{electroweak}} \approx 4 \times 10^4$. Thus, whereas the hadronic and electroweak contributions to a_e are small, those in a_μ are very significant; for this reason, a_μ is of particular interest for testing the Standard Model.

The results in Equations 18 and 19 disagree at the $3.3\text{-}\sigma$ level:

$$a_\mu^{\text{exp}} - a_\mu^{\text{theor}} = 261(80) \times 10^{-11}.$$

This discrepancy has generated wide-ranging, continuing discussion concerning the adequacy of the theory, in particular the calculation of a_μ^{hadrons} (110). It has also stimulated proposals for two new muon $g - 2$ experiments. One of these, at Fermilab, aims at reducing the uncertainty in Equation 18 by a factor of four. It will use the Brookhaven E821 storage ring but will employ new detectors, electronics, and magnetic field measurement and control, as well as a more intense and more efficiently bunched proton beam (111). Another experiment will be done at the JPARC facility in Japan (112). Here, an ultracold muon beam will be accelerated to $300 \text{ MeV}/c$ and circulated in a 66-cm-diameter storage ring. The goal is to achieve an uncertainty five times smaller than that in Equation 18.

10. THE ELECTRON ELECTRIC DIPOLE MOMENT

10.1. Electric Dipole Moments and Violation of P and T Symmetries

The electron has a spin magnetic dipole moment; can it also have a spin EDM (113)? To answer this question, we consider the Hamiltonians that describe the interactions between the spin magnetic dipole moment μ_e with a magnetic field and a hypothetical EDM d_e with an electric field. In the nonrelativistic limit, these Hamiltonians take the form

$$H_{\text{mag}} = -\mu_e \boldsymbol{\sigma} \cdot \mathbf{B}$$

and

$$H_{\text{EDM}} = -d_e \boldsymbol{\sigma} \cdot \boldsymbol{\mathcal{E}}, \quad 20.$$

where $\boldsymbol{\sigma} = \sigma_x \hat{i} + \sigma_y \hat{j} + \sigma_z \hat{k}$ and $\sigma_{x,y,z}$ are the 2×2 Pauli spin matrices. Because $\boldsymbol{\sigma}$ and \mathbf{B} are T -odd axial vectors but $\boldsymbol{\mathcal{E}}$ is a T -even polar vector, H_{mag} is invariant under P and T transformations, but H_{EDM} is odd under P and T . P is indeed violated in the weak interaction (as is C symmetry). Also, CP violation occurs in neutral K and B meson decays (114), and CP violation is equivalent to T violation if we assume CPT invariance, for which there is strong confidence. Therefore, it is possible for the weak interaction and the mechanism or mechanisms responsible for CP violation to act in concert to generate P - and T -odd radiative corrections to the ordinary P -, C -, and T -conserving electromagnetic interaction, and thereby to generate a nonzero EDM.

Unfortunately, such radiative corrections cannot be calculated with assurance because of uncertainties in the origin of CP violation. According to the Standard Model, CP violation in the electroweak sector is described phenomenologically by a single phase that appears in the CKM (Cabibbo–Kobayashi–Maskawa) quark-mixing matrix (115). The CKM matrix description gives a satisfactory account of K and B meson CP -violation data. In the Standard Model, d_e appears only at the four-loop level of perturbation theory, and there are additional suppressions (116). Thus, the Standard Model predicts that $d_e \leq 10^{-38} e \text{ cm}$, where $e = 4.8 \times 10^{-10} \text{ esu}$ is the unit of electronic charge. This value is 11 orders of magnitude smaller than the present experimental limit on d_e :

$$|d_e^{\text{exp}}| \leq 1.05 \times 10^{-27} e \text{ cm} \quad 21.$$

In fact, the Standard Model prediction is so small that if there are no other sources of CP violation, future observation of an EDM is very unlikely, given present and foreseeable experimental capabilities. However, there are good reasons to think that additional mechanisms for CP violation might exist. It is generally accepted that if the universe were initially symmetric in baryon-antibaryon number, the presently observed baryon-antibaryon asymmetry could not have developed without a much larger CP violation than is contained in the Standard Model. Also, in many theories that attempt to go beyond the Standard Model, the predicted EDMs are relatively large. For example, in various supersymmetric theories many new hypothetical particles and couplings emerge, along with new CP -violating phases (117). In many of these speculative models, the electron EDM already appears at the one-loop level, and as a result, predictions for d_e are close to the present experimental limit. This possibility provides substantial motivation for continued searches for d_e .

10.2. Proper-Lorentz-Invariant, Gauge-Invariant Electric Dipole Moment Lagrangian Density

To describe the interaction of the EDM of a relativistic spin-1/2 fermion with an electromagnetic field, it is useful to employ a gauge-invariant, proper-Lorentz-invariant effective Lagrangian density. It is convenient to start with the analogous Lagrangian density for an anomalous magnetic moment (Pauli moment) in the Dirac theory, which is given by the well-known expression

$$\mathcal{L}_{\text{Pauli}} = -\kappa \frac{\mu_B}{2} \bar{\Psi} \sigma^{\mu\nu} \Psi F_{\mu\nu}. \quad 23.$$

Here, Ψ is the Dirac field for the fermion; $\bar{\Psi} = \Psi^\dagger \gamma^0$ is the Dirac conjugate field; $\sigma^{\mu\nu} = (i/2)(\gamma^\mu \gamma^\nu - \gamma^\nu \gamma^\mu)$, where $\gamma^{\mu,\nu}$ are the usual 4×4 Dirac matrices;

$$F_{\mu\nu} = \partial_\mu A_\nu - \partial_\nu A_\mu = \begin{pmatrix} 0 & \mathcal{E}_x & \mathcal{E}_y & \mathcal{E}_z \\ -\mathcal{E}_x & 0 & -B_z & B_y \\ -\mathcal{E}_y & B_z & 0 & -B_x \\ -\mathcal{E}_z & -B_y & B_x & 0 \end{pmatrix}$$

is the electromagnetic field tensor; μ_B is the Bohr magneton; and κ is a suitable constant. In terms of \mathcal{E} and \mathbf{B} fields, Equation 23 is written as

$$\mathcal{L}_{\text{Pauli}} = \kappa \mu_B \bar{\Psi} [\boldsymbol{\Sigma} \cdot \mathbf{B} - i \boldsymbol{\alpha} \cdot \boldsymbol{\mathcal{E}}] \Psi,$$

where in the standard representation

$$\boldsymbol{\Sigma} = \begin{pmatrix} \boldsymbol{\sigma} & 0 \\ 0 & \boldsymbol{\sigma} \end{pmatrix}, \quad \boldsymbol{\alpha} = \begin{pmatrix} 0 & \boldsymbol{\sigma} \\ \boldsymbol{\sigma} & 0 \end{pmatrix}.$$

This Lagrangian density yields the single-particle Hamiltonian

$$H_{\text{Pauli}} = -\kappa \mu_B (\gamma^0 \boldsymbol{\Sigma} \cdot \mathbf{B} - i \boldsymbol{\gamma} \cdot \boldsymbol{\mathcal{E}}).$$

Both $\mathcal{L}_{\text{Pauli}}$ and H_{Pauli} are P and T invariant. We make them P and T odd by means of the replacements $\mathcal{E} \rightarrow -\mathbf{B}$ and $\mathbf{B} \rightarrow \mathcal{E}$. Alternatively, this change in $\mathcal{L}_{\text{Pauli}}$ can be achieved by replacing $\sigma^{\mu\nu}$ in Equation 23 with $i\sigma^{\mu\nu} \gamma^5$, where, as usual, $\gamma^5 = i\gamma^0 \gamma^1 \gamma^2 \gamma^3$. By making the latter transformation and replacing $\kappa \mu_B$ with d_e , we obtain the EDM Lagrangian density

$$\mathcal{L}_{\text{EDM}} = -i \frac{d_e}{2} \bar{\Psi} \sigma^{\mu\nu} \gamma^5 \Psi F_{\mu\nu} = d_e \bar{\Psi} [\boldsymbol{\Sigma} \cdot \boldsymbol{\mathcal{E}} + i \boldsymbol{\alpha} \cdot \mathbf{B}] \Psi, \quad 24.$$

which was first described by Salpeter (118). The Lagrangian density \mathcal{L}_{EDM} yields the single-particle Hamiltonian

$$H_{\text{EDM}} = -d_e(\gamma^0 \boldsymbol{\Sigma} \cdot \boldsymbol{\mathcal{E}} + i\boldsymbol{\gamma} \cdot \boldsymbol{B}). \quad 25.$$

In the nonrelativistic limit, the first term on the right-hand side of Equation 25 reduces to the right-hand side of Equation 20. However, when the fermion is relativistic, the full expression on the right-hand side of Equation 25, or at least the first term, must be used. Doing so has very significant consequences, as we describe below.

10.3. Electron Electric Dipole Moment Experimental Searches

It is impractical to search for d_e by trying to measure the spin-dependent energy of a free electron in an electrostatic field because the electron would rapidly be accelerated out of the region of observation. Although one of the first searches was done at Michigan in a special experiment utilizing free electrons (119), more recent searches have employed a more sensitive technique in which an external electrostatic field is applied to a neutral paramagnetic atom or molecule (120–127). At first glance, this approach appears useless because, in the limits where all atomic or molecular constituents are point charges and where nonrelativistic quantum mechanics applies, the atom or molecule cannot possess an EDM d_a (i.e., cannot exhibit a linear Stark effect) to first order in d_e . This is Schiff's theorem (128), which can be understood qualitatively as follows:

A neutral atom or molecule is not accelerated in a uniform external electric field. Thus, the average force on each of the atomic or molecular constituents must be zero. Because in the nonrelativistic limit all extranuclear forces are electrostatic, the average electric field at each point charge must vanish. The electric field vanishes because the external field is cancelled, on average, by the internal polarizing field.

We note in passing that Schiff's theorem does not conflict with the existence of so-called permanent EDMs of polar molecules, familiar in chemistry and molecular spectroscopy. These moments do not violate P or T , nor do they result in a linear Stark effect for sufficiently small applied electric fields, in the absence of degeneracy. They have entirely different observational signatures than exist for d_e .

In 1965, Sandars (129) showed that Schiff's theorem is evaded for a paramagnetic atom when special relativity is taken into account. He derived this important result from the first term on the right-hand side of Equation 25, including the factor γ^0 . (An intuitive explanation for this phenomenon is given in Reference 130.) Sandars's result is conveniently expressed in terms of the ratio d_a/d_e or, equivalently, in terms of the effective electric field \mathcal{E}_{eff} experienced by d_e . It is convenient to write $\mathcal{E}_{\text{eff}} = Q\Pi$, where Q is a factor that includes relativistic effects as well as details of atomic structure and Π is the degree of polarization of the atom by the external electric field \mathcal{E}_{ext} . For paramagnetic atoms with valence electrons in $s_{1/2}$ or $p_{1/2}$ orbitals, such as cesium and thallium in their ground states,

$$Q \approx 4 \times 10^{10} (Z/80)^3 \text{ V cm}^{-1}, \quad 26.$$

where Z is the atomic number. Also, for such atoms in all practical situations, $\Pi \approx 10^{-3} (\mathcal{E}_{\text{ext}}/100 \text{ keV cm}^{-1})$, which is only $\approx 10^{-3}$ for the maximum attainable laboratory field $\mathcal{E}_{\text{ext}} \approx 100 \text{ keV cm}^{-1}$. Because for paramagnetic atoms Π is proportional to \mathcal{E}_{ext} , the ratio $\mathcal{E}_{\text{eff}}/\mathcal{E}_{\text{ext}}$ is a constant and is usually known as the enhancement factor $R = d_a/d_e$. For the ground states of alkali atoms and for thallium, one finds that $|R| \approx 10Z^3\alpha^2$.

The approximate Equation 26 also applies for a wide range of heavy polar diatomic paramagnetic molecules with valence electrons in σ or π orbitals, such as YbF in the ground $^2\Sigma_{1/2}$

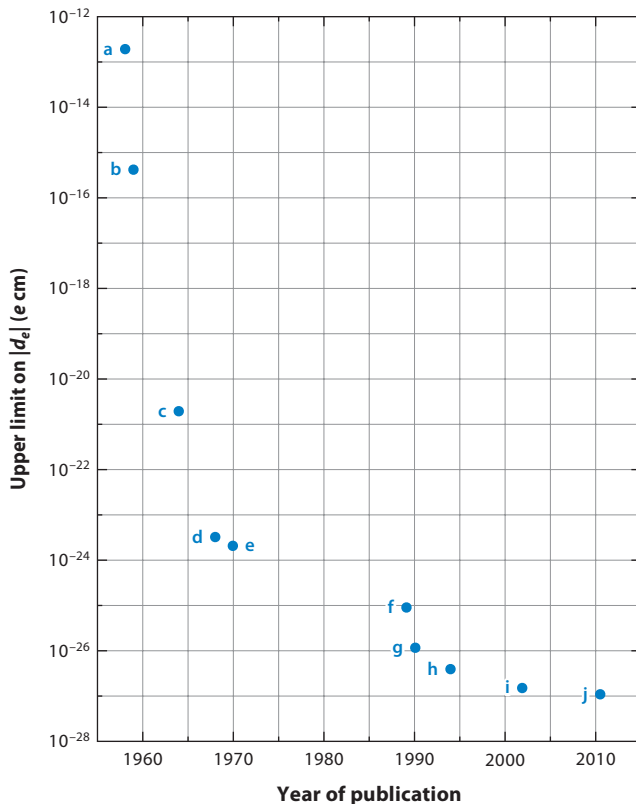


Figure 8

Experimentally determined upper limit to the electron electric dipole moment $|d_e|$ versus year of publication. Letters a through j represent References 118 through 127, respectively.

state. (In these cases, Z is the atomic number of the heavy nucleus.) The main difference between atoms and molecules appears in the factor Π . In a typical polar diatomic molecule, nearly complete polarization ($\Pi \approx 1$) can be achieved with relatively modest external electric fields ($\mathcal{E}_{\text{ext}} \approx 10^2 - 10^4 \text{ V cm}^{-1}$) because of the very close spacing between adjacent spin-rotational levels of opposite P within a given electronic state. When $\Pi \approx 1$, \mathcal{E}_{eff} is approximately three orders of magnitude larger than the maximum attainable with paramagnetic atoms. Thus, such molecules are very attractive candidates for electron EDM searches. The most sensitive search to date (and the first with a paramagnetic molecule) employed YbF in a molecular beam RF resonance experiment with laser optical pumping (127); this search obtained the limit given in Equation 21. **Figure 8** shows the limits on $|d_e|$ achieved by this and earlier experiments, plotted versus year of publication.

Experiments in which one applies a strong electric field to a suitable paramagnetic solid have also been proposed. In principle, the interaction between the EDMs of the unpaired electrons and the electric field at a sufficiently low temperature can yield a net magnetization of the sample, which can be detected by a SQUID (superconducting quantum interference magnetometer). Alternatively, application of an external magnetic field to a suitable ferrimagnetic solid can yield an EDM-induced electric polarization of the sample, which is detectable in principle by ultrasensitive charge-measurement techniques.

At present, many new experimental searches for d_e are in progress; these searches use either cesium, francium, YbF, PbO, ThO, HfF⁺, PbF, or one of numerous special solid materials. The chances are good that at least one of these searches will improve the existing limit by a factor of 10 or more in the relatively near future. At the very least, such an improvement might help narrow the field of speculation for various supersymmetric theories that attempt to go beyond the Standard Model.

11. CONCLUDING REMARKS ON SPIN

At the present stage of knowledge, the electron is considered to be a particle with no spatial extension, and the same is true of the other leptons as well as the quarks. Thus, the spin angular momentum of a fundamental fermion, an observable with no classical analog, is considered by many physicists to be describable only by abstract mathematical expressions, with no possibility of intuitive visualization. However, a contrary view was provided by Ohanian (131) in 1984, based on work by Belinfante (132) in 1939. Starting from a symmetric form of the energy-momentum tensor associated with the Dirac Lagrangian density, Ohanian showed that spin angular momentum arises from a circular flow of energy in the electron wave field, and that the intrinsic spin magnetic moment ($g_s = 2$) is associated with a similar circular flow of charge. Furthermore, by way of demonstration that these ideas are quite general, Ohanian used a symmetric form of the energy-momentum tensor for a circularly polarized Maxwell field to derive separate expressions for the orbital and spin angular momenta of that field, and thus he arrived at an intuitive picture of photon spin. Finally, in 1952 a somewhat similar analysis for the electron, expressed in terms of the zitterbewegung, was given by Huang (133).

DISCLOSURE STATEMENT

The author is not aware of any affiliations, memberships, funding, or financial holdings that might be perceived as affecting the objectivity of this review.

LITERATURE CITED

1. Jammer M. *The Conceptual Development of Quantum Mechanics*. New York: McGraw-Hill (1966)
2. Fierz M, Weisskopf VF, eds. *Theoretical Physics in the Twentieth Century: A Memorial Volume to Wolfgang Pauli*. New York: Interscience (1960)
3. Uhlenbeck GE. *Oude en nieuwe vragen der natuurkunde*. Amsterdam: North Holland (1955); Uhlenbeck GE. *Phys. Today* 29:43 (1976)
4. Goudsmit SA. *J. Phys.* 28:123 (1967); Goudsmit SA. *Phys. Today* 29:40 (1976)
5. Tomonaga S. *The Story of Spin*. Chicago: Univ. Chicago Press (1997)
6. Schweber SS. *QED and the Men Who Made It: Dyson, Feynman, Schwinger, and Tomonaga*. Princeton: Princeton Univ. Press (1994)
7. Roberts BL, Marciano WJ, eds. *Lepton Dipole Moments: Advanced Series on Directions in High Energy Physics*, vol. 20. Singapore: World Sci. (2010)
8. Roberts BL. *Annu. Rev. Nucl. Part. Sci.* 62: In press (2012)
9. Compton AH. *J. Franklin Inst.* 192:145 (1921)
10. Lande A. *Z. Phys.* 5:231 (1921); Lande A. *Z. Phys.* 5:231 (1921); Lande A. *Z. Phys.* 5:231 7:398 (1921); Lande A. *Z. Phys.* 15:189 (1923); Lande A. *Z. Phys.* 19:112 (1923)
11. Pauli W. *Z. Phys.* 31:765 (1925)
12. Pauli W. *Theory of Relativity*. New York: Pergamon (1958)
13. Uhlenbeck GE, Goudsmit SA. *Naturwissenschaften* 13:953 (1925)
14. Uhlenbeck GE, Goudsmit SA. *Nature* 117:264 (1926)

15. Thomas LH. *Nature* 117:514 (1926); Thomas LH. *Phil. Mag.* 3:1 (1927); Jackson JD. *Classical Electrodynamics*, pp. 548–53, 563–64. New York: Wiley. 3rd ed. (1998)
16. Pauli W. *Z. Phys.* 43:601 (1927)
17. Darwin CG. *Proc. R. Soc. Lond. A* 115:1 (1927); Darwin CG. *Proc. R. Soc. Lond. A* 116:227 (1927)
18. Dirac PAM. *Proc. R. Soc. Lond. A* 117:610 (1928); Dirac PAM. *Proc. R. Soc. Lond. A* 118:351 (1928)
19. Darwin CG. *Proc. R. Soc. Lond. A* 118:654 (1928); Gordon W. *Z. Phys.* 48:11 (1928)
20. Kronig R. *Nature* 117:550 (1926)
21. Pauli W. *Naturwissenschaften* 12:741 (1924)
22. Dennison DM. *Proc. R. Soc. Lond. A* 115:483 (1927)
23. Goudsmit SA. *Phys. Today* 14:6 (1961); Goudsmit SA. *Phys. Today* 14:18 (1961)
24. Fermi E. *Z. Phys.* 60:320 (1930)
25. Chadwick J. *Nature* 129:312 (1932); Chadwick J. *Proc. R. Soc. Lond. A* 136:692 (1932)
26. Iwamoto D. *Nature* 129:798 (1932)
27. Heisenberg W. *Z. Phys.* 77:1 (1932)
28. Dirac PAM. *Proc. R. Soc. Lond. A* 114:243 (1927)
29. Heisenberg W, Pauli W. *Z. Phys.* 56:1 (1929); Heisenberg W, Pauli W. *Z. Phys.* 59:168 (1930)
30. Waller I. *Z. Phys.* 61:837 (1930); Waller I. *Z. Phys.* 61:721 (1930)
31. Oppenheimer JR. *Phys. Rev.* 35:461 (1930)
32. Dirac PAM. *Proc. R. Soc. Lond. A* 126:360 (1930)
33. Oppenheimer JR. *Phys. Rev.* 35:562 (1930)
34. Tamm I. *Z. Phys.* 62:545 (1930)
35. Dirac PAM. *Proc. R. Soc. Lond. A* 133:60 (1931)
36. Anderson CD. *Phys. Rev.* 43:491 (1933)
37. Blackett PMS, Occhialini G. *Proc. R. Soc. Lond. A* 139:699 (1933)
38. Fock V. *Dokl. Akad. Nauk. USSR* 1:267 (1933)
39. Furry W, Oppenheimer JR. *Phys. Rev.* 45:245 (1934)
40. Heisenberg W. *Z. Phys.* 90:209 (1934)
41. Dirac PAM. *Theory of the positron*. Presented at Solvay Conf., 7th, Brussels (1933)
42. Weisskopf VF. *Kgl. Danske Videnskab. Selskab Mat. Fys. Medd.* 14:1 (1936)
43. Uehling EA. *Phys. Rev.* 48:55 (1935)
44. Weisskopf VF. *Z. Phys.* 89:27 (1934); Weisskopf VF. *Z. Phys.* 90:817 (1934)
45. Weisskopf VF. *Phys. Rev.* 56:72 (1939)
46. Fermi E. *Nuovo Cim.* 2:1 (1934); Fermi E. *Z. Phys.* 88:161 (1934)
47. Yukawa H. *Proc. Phys. Math. Soc. Jpn.* 17:48 (1935)
48. Pauli W. *Phys. Rev.* 58:716 (1940)
49. Rabi II. *Phys. Rev.* 51:652 (1937)
50. Estermann I, Stern O. *Z. Phys.* 85:17 (1933); Frisch R, Stern O. *Z. Phys.* 85:4 (1933)
51. Rabi II, Zacharias J, Millman S, Kusch P. *Phys. Rev.* 53:318 (1938)
52. Millman S, Kusch P. *Phys. Rev.* 60:91 (1941)
53. Nafe JE, Nelson EB, Rabi II. *Phys. Rev.* 71:914 (1947); Nafe JE, Nelson EB, Rabi II. *Phys. Rev.* 73:718 (1948)
54. Nagle DE, Julian RS, Zacharias JR. *Phys. Rev.* 72:971 (1947)
55. Breit G. *Phys. Rev.* 72:984 (1947)
56. Lamb WE, Retherford RC. *Phys. Rev.* 72:241 (1947); Lamb WE, Retherford RC. *Phys. Rev.* 79:549 (1950); Lamb WE, Retherford RC. *Phys. Rev.* 81:221 (1950)
57. Bethe HA. *Phys. Rev.* 72:339 (1947)
58. French B, Weisskopf VF. *Phys. Rev.* 75:1240 (1949)
59. Kroll NM, Lamb WE. *Phys. Rev.* 75:388 (1949)
60. Tomonaga S, Oppenheimer JR. *Phys. Rev.* 74:224 (1948)
61. Schwinger J. *Phys. Rev.* 73:416 (1948); Schwinger J. *Phys. Rev.* 76:790 (1949)
62. Kusch P, Foley HM. *Phys. Rev.* 72:1256 (1947); Kusch P, Foley HM. *Phys. Rev.* 74:250 (1948)
63. Feynman RP. *Phys. Rev.* 74:1430 (1948); Feynman RP. *Phys. Rev.* 76:749 (1949); Feynman RP. *Phys. Rev.* 76:769 (1949)

64. Schwinger J. *Phys. Rev.* 74:1439 (1948); Schwinger J. *Phys. Rev.* 75:651 (1949); Schwinger J. *Phys. Rev.* 75:898 (1949); Schwinger J. *Phys. Rev.* 76:790 (1949)
65. Dyson FJ. *Phys. Rev.* 75:486 (1949)
66. Dyson FJ. *Phys. Rev.* 75:1736 (1949)
67. Salam A. *Phys. Rev.* 82:217 (1951)
68. Ward JC. *Proc. R. Soc. Lond. A* 64:54 (1951)
69. Koenig S, Prodel AS, Kusch P. *Phys. Rev.* 83:687 (1951); Koenig S, Prodel AS, Kusch P. *Phys. Rev.* 88:191 (1952)
70. Beringer R, Heald M. *Phys. Rev.* 95:1474 (1954)
71. Gardner JH, Purcell EM. *Phys. Rev.* 76:1262 (1949)
72. Liebes S, Franken P. *Phys. Rev.* 116:633 (1959)
73. Schupp AA, Pidd RW, Crane HR. *Phys. Rev.* 121:1 (1961)
74. Wilkinson DT, Crane HR. *Phys. Rev.* 130:852 (1963)
75. Wesley JC, Rich A. *Phys. Rev. A* 4:1341 (1971)
76. Rich A, Crane HR. *Phys. Rev. Lett.* 17:271 (1966)
77. Gilleland JR, Rich A. *Phys. Rev. A* 5:38 (1972)
78. Van Dyck RS Jr, Schwinberg PB, Dehmelt HG. *Phys. Rev. Lett.* 59:26 (1987)
79. Brown LS. *Phys. Rev. Lett.* 52:2013 (1984); Brown LS. *Ann. Phys. A* 159:62 (1985)
80. Odum B, Hanneke D, D'Urso B, Gabrielse G. *Phys. Rev. Lett.* 97:030801 (2006)
81. Hanneke D, Fogwell S, Gabrielse G. *Phys. Rev. Lett.* 100:120801 (2008)
82. Karplus R, Kroll NM. *Phys. Rev.* 77:536 (1950)
83. Petermann A. *Helv. Phys. Acta* 30:407 (1957)
84. Sommerfield C. *Phys. Rev.* 107:328 (1957); Sommerfield C. *Ann. Phys.* 5:26 (1958)
85. Suura H, Wichmann E. *Phys. Rev.* 105:1930 (1957)
86. Petermann A. *Phys. Rev.* 105:1931 (1957)
87. Laporta S, Remiddi E. *Phys. Lett. B* 379:283 (1996)
88. Laporta S, Remiddi E. See Ref. 7, chapter 4 (2010)
89. Kinoshita T. *Phys. Rev. Lett.* 75:4728 (1995)
90. Kinoshita T. See Ref. 7, chapter 4 (2010)
91. Aoyama T, et al. *Phys. Rev. Lett.* 99:110406 (2007); Aoyama T, et al. *Phys. Rev. D* 77:053012 (2008)
92. Nio M, et al. *Nucl. Phys. B Proc. Suppl.* 169:238 (2007)
93. Aoyama T, et al. *Phys. Rev. D* 78:113006 (2008); Aoyama T, et al. *Phys. Rev. D* 81:053009 (2010); Aoyama T, et al. *Phys. Rev. D* 82:113004 (2010); Aoyama T, et al. *Phys. Rev. D* 83:053002 (2011); Aoyama T, et al. *Phys. Rev. D* 83:053003 (2011)
94. Davier M, Eidelman S, Hocker A, Zhang Z. *Euro. Phys. J. C* 31:503 (2003)
95. Davier M. See Ref. 7, chapter 8 (2010)
96. de Rafael E. *Phys. Lett. B* 322:239 (1994)
97. Bijnens J, Pallante E, Prades J. *Phys. Rev. Lett.* 75:1447 (1995); Bijnens J, Pallante E, Prades J. *Phys. Rev. Lett.* 75:3781 (1995)
98. Prades J, Rafael E, Vainshtein A. See Ref. 7, chapter 9 (2010)
99. Czarnecki A, Marciano WJ. See Ref. 7, chapter 2 (2010)
100. Fujikawa K, Lee BW, Sanda AI. *Phys. Rev. D* 6:2923 (1972); Jackiw R, Weinberg S. *Phys. Rev. D* 5:2473 (1972); Altarelli G, Cabibbo N, Maiani L. *Phys. Lett. B* 40:415 (1972); Bars I, Yoshimura M. *Phys. Rev. D* 6:374 (1972); Bardeen WA, Gastmans R, Lautrup BE. *Nucl. Phys. B* 46:315 (1972)
101. Kukhto TV, Kuraev EA, Schiller A, Silagadze ZK. *Nucl. Phys. B* 371:567 (1992); Czarnecki A, Krause B, Marciano WJ. *Phys. Rev. Lett.* 76:3267 (1996); Czarnecki A, Marciano WJ, Vainshtein A. *Phys. Rev. D* 67:073006 (2003)
102. Wicht A, Hensley JM, Sarajlic E, Chu S. *Phys. Scr. T* 102:82 (2002)
103. Cadoret M, et al. *Phys. Rev. Lett.* 101:230801 (2008)
104. Gabrielse G. See Ref. 7, chapter 6 (2010)
105. Pachucki K, Sapirstein J. See Ref. 7, chapter 7 (2010)
106. Smiciklas M, Shiner D. *Phys. Rev. Lett.* 105:123001 (2010)

107. Pachucki K, Yerokhin VA. *Phys. Rev. Lett.* 104:070403 (2010)
108. Bennett G, et al. [Muon ($g-2$) Collab.] *Phys. Rev. D* 73:072003 (2006); Bennett G, et al. [Muon ($g-2$) Collab.] *Phys. Rev. Lett.* 92:161802 (2004)
109. Miller JP, Roberts BL, Jungmann K. See Ref. 7, chapter 11 (2010)
110. Hagiwara K, et al. *J. Phys. G* 38:085003 (2011)
111. Roberts BL. [New Muon ($g-2$) Collab.] *Chin. Phys. C* 34:741 (2010)
112. Mibe T. [J-PARC ($g-2$) Collab.] *Chin. Phys. C* 34:745 (2010)
113. Commins ED, DeMille D. See Ref. 7, chapter 14 (2010)
114. Kirkby D, Nir Y. In *Review of Particle Physics*, ed. WM Yao, et al., p. 145. Berkeley: Lawrence Berkeley Lab. (2006)
115. Hocker A, Ligeti Z. *Annu. Rev. Nucl. Part. Sci.* 56:501 (2006)
116. Pospelov M, Khriplovich IB. *Sov. J. Nucl. Phys.* 53:638 (1991)
117. Pospelov M, Ritz A. See Ref. 7, chapter 13 (2010)
118. Salpeter EE. *Phys. Rev.* 112:1642 (1958)
119. Nelson DF, Schupp AA, Pidd RW, Crane HR. *Phys. Rev. Lett.* 2:492 (1959)
120. Sandars PGH, Lipworth E. *Phys. Rev. Lett.* 13:529 (1964); Sandars PGH, Lipworth E. *Phys. Rev. Lett.* 14:718 (1964); Sandars PGH. *J. Phys. B* 1:494 (1968); Sandars PGH. *J. Phys. B* 1:511 (1968)
121. Weisskopf MC, et al. *Phys. Rev. Lett.* 19:741 (1967); Weisskopf MC, et al. *Phys. Rev.* 174:125 (1968)
122. Player MA, Sandars PGH. *J. Phys. B* 3:1620 (1970)
123. Murthy SA, Krause D, Li L, Hunter LR. *Phys. Rev. Lett.* 63:965 (1989)
124. Abdullah K, et al. *Phys. Rev. Lett.* 65:2347 (1990)
125. Commins ED, Ross SB, DeMille D, Regan BC. *Phys. Rev. A* 50:2960 (1994)
126. Regan BC, Commins ED, Schmidt CJ, DeMille D. *Phys. Rev. Lett.* 88:071805 (2002)
127. Hudson JJ, et al. *Nature* 473:493 (2011)
128. Schiff LI. *Phys. Rev.* 132:2194 (1963)
129. Sandars PGH. *Phys. Lett.* 14:194 (1965); Sandars PGH. *Phys. Lett.* 22:290 (1966)
130. Commins ED, Jackson JD, DeMille DP. *Am. J. Phys.* 75:532 (2007)
131. Ohanian HC. *Am. J. Phys.* 54:500 (1984)
132. Belinfante FJ. *Physica* 6:887 (1939)
133. Huang K. *Am. J. Phys.* 20:479 (1952)



Contents

Puzzles in Hadronic Physics and Novel Quantum Chromodynamics Phenomenology <i>Stanley J. Brodsky, Guy de Téramond, and Marek Karliner</i>	1
The Casimir Force and Related Effects: The Status of the Finite Temperature Correction and Limits on New Long-Range Forces <i>Steve K. Lamoreaux</i>	37
Backreaction in Late-Time Cosmology <i>Thomas Buchert and Syksy Räsänen</i>	57
Supernova Neutrino Detection <i>Kate Scholberg</i>	81
The CLIC Study of a Multi-TeV Linear Collider <i>J.P. Delahaye</i>	105
Electron Spin and Its History <i>Eugene D. Commins</i>	133
Chiral Dynamics of Few- and Many-Nucleon Systems <i>Evgeny Epelbaum and Ulf-G. Meißner</i>	159
Next-to-Leading-Order Event Generators <i>Paolo Nason and Bryan Webber</i>	187
Neutrino Masses from the Top Down <i>Paul Langacker</i>	215
Muon ($g - 2$): Experiment and Theory <i>James P. Miller, Eduardo de Rafael, B. Lee Roberts, and Dominik Stöckinger</i>	237
Twenty-First Century Lattice Gauge Theory: Results from the Quantum Chromodynamics Lagrangian <i>Andreas S. Kronfeld</i>	265
M-Theory and Maximally Supersymmetric Gauge Theories <i>Neil Lambert</i>	285

Results from the Borexino Solar Neutrino Experiment <i>Frank Calaprice, Cristiano Galbiati, Alex Wright, and Aldo Ianni</i>	315
Parity-Violating Electron Scattering and the Electric and Magnetic Strange Form Factors of the Nucleon <i>D.S. Armstrong and R.D. McKeown</i>	337
First Results from Pb+Pb Collisions at the LHC <i>Berndt Müller, Jürgen Schukraft, and Bolesław Wysłouch</i>	361
Hard Processes in Proton-Proton Collisions at the Large Hadron Collider <i>Jonathan M. Butterworth, Günther Dissertori, and Gavin P. Salam</i>	387
Explosion Mechanisms of Core-Collapse Supernovae <i>Hans-Thomas Janka</i>	407
The Underlying Event in Hadronic Collisions <i>Rick Field</i>	453
The Nuclear Equation of State and Neutron Star Masses <i>James M. Lattimer</i>	485

Indexes

Cumulative Index of Contributing Authors, Volumes 53–62	517
Cumulative Index of Chapter Titles, Volumes 53–62	521

Errata

An online log of corrections to *Annual Review of Nuclear and Particle Science* articles may be found at <http://nucl.annualreviews.org/errata.shtml>